HAL
open science

Targeted deletion of kidney glucose-6 phosphatase leads to nephropathy.

Julie Clar, Blandine Gri, Julien Calderaro, Marie-Christine Birling, Yann Herault, Peter G Smith, Gilles Mithieux, Fabienne Rajas

To cite this version:

Julie Clar, Blandine Gri, Julien Calderaro, Marie-Christine Birling, Yann Herault, et al.. Targeted deletion of kidney glucose-6 phosphatase leads to nephropathy.. Kidney International, 2014, 86 (4), pp.747-756. 10.1038/ki.2014.102 . inserm-01350891

HAL Id: inserm-01350891

https://inserm.hal.science/inserm-01350891v1

Submitted on 2 Aug 2016

HAL is a multi-disciplinary open access archive for the deposit and dissemination of scientific research documents, whether they are published or not. The documents may come from teaching and research institutions in France or abroad, or from public or private research centers.

L'archive ouverte pluridisciplinaire **HAL**, est destinée au dépôt et à la diffusion de documents scientifiques de niveau recherche, publiés ou non, émanant des établissements d'enseignement et de recherche français ou étrangers, des laboratoires publics ou privés.

Kidney-targeted deletion of glucose-6 phosphatase leads to nephropathy

Julie Clar[1-3], Blandine Gri[1-3], Julien Calderaro[4], Marie-Christine Birling[5], Yann Hérault[5], G. Peter. A. Smit[6], Gilles Mithieux[1-3] & Fabienne Rajas[1-3]

[1]Institut National de la Santé et de la Recherche Médicale, U855, Lyon, F-69008, France

[2]Université de Lyon, Lyon, F-69008 France

[3]Université Lyon1, Villeurbanne, F-69622 France

[4]Département de Pathologie, Hôpital Henri Mondor, Créteil, France

[5]Institut Clinique de la Souris, Illkirch, France

[6]Universitair Medisch Centrum Groningen, NL-9713 Groningen, The Netherlands

Address for correspondence: Dr. Fabienne Rajas

Inserm U855, Faculté de Médecine Laennec

7 rue Guillaume Paradin, 69372 Lyon cedex 08 France

Tel: 33 478 77 10 28/Fax: 33 478 77 87 62

E-mail: fabienne.rajas@univ-lyon1.fr

Running title: **Specific renal loss of G6Pase leads to nephropathy**

Word count: 3942 words

Abstract: 1469 characters

Number of tables and figures: 5 figures + 2 tables + 1 supplementary table+ 1 supplemental figure

ABSTRACT

Renal failure is a major complication that arises with aging in glycogen storage disease type 1a and type 1b patients. In the kidneys, glucose-6 phosphatase catalytic subunit (encoded by *G6pc*) deficiency leads to the accumulation of glycogen; this effect results in marked nephromegaly and progressive glomerular hyperperfusion and hyperfiltration, which precede the development of microalbuminuria and proteinuria. To better understand the end-stage nephropathy in glycogen storage disease type 1a, we generated a novel kidney-specific *G6pc* knock-out (K-G6pc$^{-/-}$) mouse, which exhibited normal life expectancy. After 6 months of *G6pc* deficiency, K-G6pc$^{-/-}$ mice showed glycogen overload leading to nephromegaly and tubular dilation. Moreover, renal accumulation of lipids due to activation of *de novo* lipogenesis was observed. This led to the activation of the renin-angiotensin system and the development of epithelial-mesenchymal transition process and podocyte injury *via* transforming growth factor β1 signaling. Thus, K-G6pc$^{-/-}$ mice developed microalbuminuria caused by the impairment of glomerular filtration barrier. In conclusion, renal *G6pc* deficiency alone is sufficient to induce the development of the early onset nephropathy observed in glycogen storage disease type 1a, independently of the liver disease. K-G6pc$^{-/-}$ mouse model is a unique tool to decipher the molecular mechanisms underlying renal failure and to evaluate potential therapeutic strategies.

Keywords : Glycogen storage disease, nephropathy, gluconeogenesis, microalbumineria, epithelial-mesenchymal transition, podocyte injury, TGF-β1

Glycogen storage disease (GSD) type 1 is an inherited disease characterized by severe hypoglycemia associated with hepatic, renal and intestinal disorders. GSD type 1 is caused by a deficiency in glucose-6-phosphatase (G6Pase) activity, a key enzyme in endogenous glucose production[1,2]. G6Pase catalyzes the hydrolysis of glucose-6-phosphate (G6P), the terminal step of glucose production common to glycogenolysis and gluconeogenesis. GSD type 1a (GSD1a, OMIM ♯232200） is caused by mutations affecting the catalytic subunit (G6PC) of the G6Pase complex[3,4]. G6PC is specifically expressed in the liver, kidneys and intestines, which are the only organs capable of producing glucose in the blood[5–7]. In the kidney, the gluconeogenic function is restricted to the proximal convoluted tubules of the cortex[8]. The clinical manifestations in GSD1 patients are fasting hypoglycemia, growth retardation, hypertriglyceridemia, hypercholesterolemia, hyperuricemia, hypoketonemia and lactic acidemia[9]. Moreover, G6Pase deficiency leads to the accumulation of G6P and glycogen in hepatocytes and proximal renal tubules that results in hepatomegaly and nephromegaly, respectively. Since the 1980s, the life expectancy of GSD1 patients has been considerably improved by dietary management to achieve suitable metabolic control[10,11]. However, various complications occur with aging, such as gouty arthritis, osteoporosis, pulmonary hypertension, hepatic tumors and progressive chronic renal disease[12–14]. Renal failure is one of the main causes of morbidity in GSD1 patients with aging.

Although renal disease was mentioned in von Gierke's original pathological description, the chronic renal disease of GSD1a was later recognized as a major complication[15,16]. Nearly all GSD1 patients above 25 years of age exhibit renal disease with microalbuminuria, and more than 50% exhibit proteinuria[12]. The first manifestation is glomerular hyperperfusion and hyperfiltration before the development of microalbuminuria

and then proteinuria[17]. In addition, some patients also develop hypertension and nephrocalcinosis due to hyperuricemia, hypercalciuria and hypocitraturia. At a later stage, kidney failure occurs, which can require dialysis or even renal transplantation[12,13]. In addition, renal biopsies reveal tubular atrophy, glomerulosclerosis and interstitial fibrosis[17–20]. Recent molecular studies suggest the involvement of the renin-angiotensin system in the development of renal fibrosis and renal oxidative stress in total *G6pc* knock-out mice[21,22]. Accordingly, treatment with inhibitors of angiotensin converting enzyme (ACE) and/or angiotensin II receptor antagonists partially corrects glomerular filtration in GSD1 patients, but no significant effect is observed on microalbuminuria and proteinuria[23,24]. Therefore, further investigations are needed to better understand the long-term mechanisms of the renal disease and to evaluate potential therapeutic strategies. Unfortunately, the long-term renal complications cannot be evaluated using total *G6pc* knock-out mice because they rarely survive over weaning, which is likely due to the concomitant liver disease[25].

To investigate the onset of GSD1 renal pathology independently of liver disease, we generated a novel GSD1a mouse model that exclusively targets G6PC deletion in the kidneys. We used a CRE-lox approach similar to that used to generate the liver-deficient model[26]. The kidney-specific *G6pc* knock-out (K-G6pc$^{-/-}$) mice are viable and develop renal symptoms similar to the human pathology. This novel mouse model allows us to elucidate new molecular pathways involved in the impairment of the glomerular filtration barrier, such as podocyte alterations and ChREBP activation, which leads to lipid deposits.

RESULTS

Generation of mice with kidney-specific G6Pase deficiency

We generated mice lacking G6PC specifically in the kidneys by an inducible CRE-lox strategy. As the renal *G6pc* expression is restricted to the proximal tubules of the cortex region[8], we used mice expressing the inducible CRE^{ERT2} recombinase under the control of the kidney androgen regulated protein (Kap) promoter. The Kap promoter is known to be specifically active in the proximal tubules of the kidney where it is inducible by androgen[27]. Male B6.$G6pc^{lox/lox}$.$Kap^{creERT2/w}$ mice were treated with tamoxifen at 6-8 weeks of age to induce the excision of *G6pc* exon 3 in the kidneys.

PCR analysis of purified DNA showed a tissue-specific deletion of *G6pc* exon 3 in the kidneys of K-$G6pc^{-/-}$ mice (Figure 1A). The kidney-specific expression of CRE^{ERT2} recombinase under the control of the Kap promoter was confirmed by the presence of full length *G6pc* in the liver, intestine, testis and epididymis (Figure 1A). However, *G6pc* exon 3 deletion was only partial, since a floxed fragment of 1189 bp was also amplified in the kidneys of K-$G6pc^{-/-}$ mice (Figure 1A). This deletion was sufficient to inhibit G6Pase activity by about 50% in the kidneys of K-$G6pc^{-/-}$ mice compared to WT mice (Figure 1B). Western blot analyses confirmed the marked decrease in G6PC protein levels in K-$G6pc^{-/-}$ kidneys (Figure 1B). As expected, G6Pase expression is restricted to the proximal convoluted tubules of the cortex in WT mice (Figure 1C&E). In contrast, K-$G6pc^{-/-}$ kidneys showed a lower and heterogeneous immunostaining for G6PC in the cortex (Figure 1D&F), with the presence of only a few G6PC positive cells identified as proximal convoluted tubules (Supplemental Figure 1). G6PC was not detectable in the medulla, distal convoluted tubules or glomeruli in both WT and K-$G6pc^{-/-}$ mice (Figure 1C-D).

Metabolic, morphological and molecular characterization of the kidney disease in K-$G6pc^{-/-}$ mice

In contrast to the growth retardation reported in total *G6pc* knock-out mice[25], the 6 month renal *G6pc* deficiency that was induced at adulthood did not affect body weight (Table 1). K-G6pc$^{-/-}$ mice were viable without treatment and were normoglycemic after 6 h of fasting (Table 1). The liver weight was similar in K-G6pc$^{-/-}$ and WT mice, but hepatic G6Pase activity was increased by 40% in K-G6pc$^{-/-}$ mice compared to WT mice (Table 1). Biochemical analyses revealed normal plasma cholesterol, triglycerides, lactate and blood urea nitrogen levels in K-G6pc$^{-/-}$ mice, indicating normal liver metabolism. Interestingly, plasma uric acid concentrations were slightly higher in K-G6pc$^{-/-}$ mice compared to WT mice (Table 1).

As expected, K-G6pc$^{-/-}$ mice showed enlarged kidneys (Figure 2A-C). After 6 months, K-G6pc$^{-/-}$ kidneys accounted for about 1.72±0.06% of total body mass versus only 1.01±0.01% in WT mice (Figure 2C). This was associated with a marked glycogen accumulation in the tubules in the external part of the kidney cortex, as revealed by a periodic acid-Schiff stain (Figure 2E). Indeed, the deposition of glycogen was nearly absent in the kidneys of WT mice (Figure 2D-F) compared to 22.7±2.3 mg of glycogen/g of tissue in the K-G6pc$^{-/-}$ kidneys (Figure 2F).

Histological observations of WT kidneys by H&E staining revealed normal morphology with recognizable glomeruli (G), proximal convoluted tubules (PC) and distal convoluted tubules (DC) in the cortex (Figure 3A-C). In contrast, K-G6pc$^{-/-}$ mice showed morphological alterations in the kidney cortex with a clarification and enlargement of tubular epithelial cells (Figure 3B-D). Moreover, the abundance of renal mRNA for podocyte marker proteins such as podocin (*Nphs2*), synaptopodin (*Synpo*) and podocalyxin (*Podxl*) was decreased by 50% to 75% in K-G6pc$^{-/-}$ mice compared to WT mice (Figure 3E). Western blotting revealed a decrease in podocin (NPHS2) and nephrin protein levels in K-G6pc$^{-/-}$ kidneys. These alterations of renal morphology and podocyte damage in K-G6pc$^{-/-}$ mice were associated with disturbed urine parameters. The urinary pH of K-G6pc$^{-/-}$ mice was more acidic than that

of WT mice. Uric acid levels were also increased by 3-fold in the urine of K-G6pc$^{-/-}$ mice compared to WT mice (Table 2). Interestingly, 6 months of renal *G6pc* knock-out led to increased albuminuria but did not affect proteinuria. In addition, there was an imbalance in urinary excretion of electrolytes (Table 2). The urine magnesium and phosphate concentrations were increased in the urine of K-G6pc$^{-/-}$ mice compared to WT mice (Table 2). No difference was observed in urine potassium, sodium, chloride, calcium, oxalate or glucose concentrations (Table 2). Surprisingly, K-G6pc$^{-/-}$ mice showed hypercitraturia (Table 1) and no microlithiasis was observed. In addition, no change in urine excretion, urea level, ketone bodies level or creatinuria was observed in K-G6pc$^{-/-}$ mice compared to WT mice (Table 2).

These results showed that K-G6pc$^{-/-}$ mice exhibited profound alterations of the urinary filtration barrier leading to development of microalbumineria and electrolyte imbalance.

Epithelial-mesenchymal transition mediated *via* the activation of the renin-angiotensin system in K-G6pc$^{-/-}$ mice

We next analyzed the molecular pathways that could lead to podocyte damage and kidney injury in K-G6pc$^{-/-}$ mice. As in total *G6pc* knock-out mice, the kidneys of K-G6pc$^{-/-}$ mice showed a 2-fold increase in angiotensinogen (*Agt*) mRNA, associated to a 3-fold increase of the transforming growth factor β1 (*Tgfb1*) expression (Figure 4A). TGF-β1 inhibits the growth of most cell types, including epithelial cells, but stimulates the growth of certain mesenchymal cells[28]. In agreement with that, K-G6pc$^{-/-}$ kidneys expressed lower mRNA levels of specific epithelial proteins such as E-cadherin (*Cdh1*), tight junction protein 1 (*ZO1*) and β1-catenin (*Ctnnb1*) (Figure 4B). E-cadherin and β1-catenin proteins were decreased in K-G6pc$^{-/-}$ kidneys. In addition to the loss of epithelial markers, the expression of the

mesenchymal marker fibronectin was induced in K-G6pc$^{-/-}$ kidneys (Figure 4B). However, the abundance of others mRNAs associated with a mesenchymal phenotype such as α2 smooth muscle actin (*αSMA*), plasminogen activator inhibitor type 1 (*PAI1*) and vimentin (*Vim*) was similar in K-G6pc$^{-/-}$ and WT mice (Figure 4B). Vimentin protein levels were similar in K-G6pc$^{-/-}$ and WT kidneys (Figure 4B).

These data suggest K-G6pc$^{-/-}$ kidneys presented epithelial-mesenchymal transition (EMT)-like changes, highlighted by the loss of epithelial markers and the over-expression of fibronectin. However, no modification of the thickness of basement membrane or glomerulosclerosis was observed by electron microscopy (Figure 4C-F), suggesting that K-G6pc$^{-/-}$ showed early stage of EMT.

Lastly, K-G6pc$^{-/-}$ mice exhibited a significant increase in the mRNA levels of the proinflammatory cytokine Tnf-α, which reflected an inflammatory state (Figure 4G).

Increased triglyceride synthesis in K-G6pc$^{-/-}$ kidneys

As the accumulation of intracellular G6P activates *de novo* lipogenesis in GSD1a liver, we analyzed lipid metabolism in GSD1a kidneys. In K-G6pc$^{-/-}$ mice, Sudan red staining revealed lipid deposits in the internal part of the renal cortex (Figure 5B-C), while no staining was observed in WT kidneys (Figure 5A). In line with the accumulation of lipids, the renal expression of fatty acid synthase (*Fasn*) and acetyl-coenzyme A carboxylase α (*Acaca*), two key enzymes in fatty acid synthesis, was about 3-fold higher in K-G6pc$^{-/-}$ mice than in WT mice (Figure 5D). This could be related to the 2-fold increased expression of the transcription factor carbohydrate responsive element-binding protein (*Chrebp*), a known activator of lipogenesis gene expression (Figure 5D). No modification was observed in the levels of stearoyl-coenzyme A desaturase 1 (*Scd1*) or sterol regulatory element-binding factor 1

(*Srebf1*) mRNA (Figure 5D). Renal *G6pc* deficiency did not affect cholesterol synthesis, demonstrated by a similar expression of sterol regulatory element-binding factor 2 (*Srebf2*) and HMG coenzyme A reductase (*Hmgcr*) in K-G6pc$^{-/-}$ and WT kidneys (Figure 5D). Interestingly, K-G6pc$^{-/-}$ kidneys showed a 10-fold increase in the expression of HMG coenzyme A synthase 2 (*Hmgcs2*), the rate-limiting enzyme involved in ketogenesis (Figure 5D). This was not associated with an increase in plasmatic or urinary ketone bodies (Tables 1 and 2).

DISCUSSION

In patients with GSD1, clinical and biochemical abnormalities are improved by intensive dietary management, but various complications occur with aging. To improve our understanding of the long-term renal complications, we generated a novel GSD1a mouse model in which G6PC deletion was restricted to the kidney (K-G6pc$^{-/-}$ mice). In contrast to total *G6pc* knock-out mice, K-G6pc$^{-/-}$ mice generally survived without treatment. This allowed us to study the renal GSD1 pathology after 6 months of *G6pc* deficiency, matching the early adult age in GSD1a patients. Moreover, these mice were normoglycemic in the fed and post-absorptive states. This can be explained by only a partial suppression of renal G6Pase activity in K-G6pc$^{-/-}$ mice. Concomitantly, hepatic G6Pase activity was increased by 40%, which suggested that an increase in liver glucose production compensated the partial deficiency in the kidney.

Interestingly, the K-G6pc$^{-/-}$ mice exhibited the main symptoms of GSD1a renal disease. As previously described in GSD1 patients[19,29] and in total *G6pc* knock-out mice[21,25], renal *G6pc* deficiency led to excessive glycogen accumulation resulting in nephromegaly. After 6 months of *G6pc* deletion, K-G6pc$^{-/-}$ mice presented early renal perturbations similar to those

observed in GSD1a patients, namely microalbuminuria and hyperphosphaturia[30,31]. Despite the absence of liver deficiency, K-G6pc$^{-/-}$ mice also manifested a mild increase in plasma uric acid concentrations associated with an increase in uric acid excretion. This hyperuricemia might be explained by an increase of renal purine synthesis, driven by the up-regulation of the pentose-phosphate pathway by high intracellular levels of G6P, rather than by a defect in uric acid excretion. Although uric acid and lactate share the same transporter, K-G6pc$^{-/-}$ mice presented normal plasma lactate. This was likely due to an increased utilization of lactate by liver gluconeogenesis (see above). Moreover, no nephrolithiasis was observed in K-G6pc$^{-/-}$ mice, which was in line with normal urine calcium and oxalate concentrations. Contrarily to GSD1a patients with nephrolithiasis who have hypercalciuria and hypocitraturia[32], K-G6pc$^{-/-}$ mice presented hypercitraturia, which could protect mice from the development of calcium stone. Therefore, these results suggest that renal *G6pc* deficiency *per se* was sufficient to induce the development of a renal pathology that was independent of liver-derived metabolic changes. This was an important finding in the context of the pathophysiological concept of the GSD1 disease as a whole, but also in terms of transplantation and gene therapy. Kidney transplantation is performed in the case of severe renal failure, but this does not affect hypoglycemia[33]. In contrast, liver transplantation has been used to correct hypoglycemia and all liver-related biochemical abnormalities in GSD1 patients, but any beneficial renal effects remain to be proven[34–37]. Immunosuppressive therapy may worsen the renal disease, which may be related to cyclosporine toxicity[38]. Hence, combined liver-kidney graft should be preferred to single-organ grafts. In line with this proposal, a combined graft has been successfully performed in a few GSD1 patients whose renal function was already compromised[39,40]. Concerning gene therapy, it was shown that AAV8-treated animals presented a complete normalization of

hepatic G6PC deficiency but continued manifesting nephromegaly[41,42]. On the other hand, AAV1 or AAV2/9 vectors are able to transduce both the liver and kidneys and prevent hypoglycemia, hepatomegaly and nephromegaly[42,43]. These vectors seem be a better choice for GSD1a gene therapy but it was striking that the renal pathology was only partially improved after 12 months of AAV treatment and the gradual lost of transgene remains a significant challenge for gene therapy[42].

The predominant pathological lesion found in the K-G6pc$^{-/-}$ kidney was tubular dilation due to the massive accumulation of glycogen. In addition, K-G6pc$^{-/-}$ mice presented alterations of podocytes, revealed by down-regulation of podocyte-specific proteins such as nephrin, podocin, podocalyxin and synaptopodin. Podocytes line the outer layer of the glomerular basement membrane and form the final barrier to protein loss; thus, podocyte injury is typically associated with albuminuria or proteinuria[44–47]. Moreover, in addition to tubular epithelial cells, podocytes and endothelial cells are capable of entering the EMT process after progressive renal injury, leading to tubulointerstitial fibrosis[48,49]. The loss of epithelial adhesion represents the beginning of a series of events culminating in EMT phenotype[50]. Accordingly, K-G6pc$^{-/-}$ mice presented a decrease in epithelial marker mRNAs as E-cadherin, tight junction protein ZO-1 and β1-catenin. Changes in E-cadherin expression are rapidly accompanied by an up-regulation of mesenchymal markers[50]. Interestingly, K-G6pc$^{-/-}$ mice showed increased synthesis of fibronectin, which rapidly appears when the fibrillar extracellular matrix is formed[28]. As the excessive deposition of matrix is the hallmark of renal fibrosis, we hypothesize a possible late development of fibrosis in K-G6pc$^{-/-}$ kidneys, as observed in patients with GSD1a[16,51].

It is widely recognized that the profibrotic cytokine transforming growth factor β1 (TGFβ1) is involved in podocyte injury and in the EMT process, leading to fibrosis[28,44,45,48–50].

An increased expression of TGFβ1 in tubular epithelial cells was once reported in a GSD-1a patient exhibiting proteinuria, tubular atrophy and interstitial fibrosis[29]. Accordingly, K-G6pc$^{-/-}$ mice showed an increase in TGFβ1 expression and an activation of the renin-angiotensin system, as described in diabetes[21,52]. Indeed, angiotensin II, which is produced from angiotensinogen, is well known to increase the expression of TGFβ1[50]. Interestingly, the activation of the renin-angiotensin system is associated with the activation of protein kinase C by diacyl glycerol (DAG)[53]. A possible common denominator for both diseases could be the increased levels of G6P, which is associated with the up-regulation of the pentose-phosphate pathway. This generates NADPH for *de novo* lipogenesis, triglycerides and lipid metabolites such as DAG. Accordingly, diabetic nephropathy is associated with the presence of lipid deposits in glomeruli and proximal tubules[54]. However, little is known about renal lipid metabolism and renal lipid deposits in GSD1. To date, only one study describes the presence of lipid deposits in the kidneys of two GSD1 patients with proteinuria[51]. It is noteworthy that K-G6pc$^{-/-}$ mice presented lipid deposits in the internal part of the renal cortex, which was associated with an increased expression of key lipogenic genes, namely *Fasn* and *Acaca*. In contrast to diabetic nephropathy[55,56], renal lipid accumulation in K-G6pc$^{-/-}$ kidneys did not seem to be mediated by SREBP1 or SREBP2 but rather by the transcription factor ChREBP (Figure 5). Lastly, the excessive ketogenic activity in diabetic kidneys is associated with TGFβ1 expression and the EMT process[57]. In contrast, the ability of GSD1a patients to produce ketone bodies during fasting is controversial[58]. It is noteworthy that K-G6pc$^{-/-}$ kidneys exhibited increased ketogenic activity highlighted by the increased HMGCS2 expression. However, this did not result in an increase in ketone bodies in the plasma or urine of K-G6pc$^{-/-}$ mice. This could be due to the high capacity of the kidney to derive energy from ketone bodies, particularly under conditions of low plasma glucose[59].

In conclusion, we report the characterization of a novel mouse model of GSD1a nephropathy. We demonstrate that K-G6pc$^{-/-}$ mice develop early onset nephropathy due to the renal accumulation of G6P; this activates the pentose phosphate pathway and *de novo* lipogenesis, resulting in triglyceride accumulation. Following the activation of renin-angiotensin system, a TGFβ1 increase leads the development of EMT process and podocyte injury, resulting in impaired glomerular filtration barrier and microalbuminuria in K-G6pc$^{-/-}$ mice. Thus, this novel mouse model could be a useful tool in future studies of the pharmacological treatment of EMT and/or kidney failure. Lastly, our data firmly establish that renal *G6pc* deficiency *per se* is sufficient to induce the development of the renal pathology, independently of the liver disease. These results also suggest that a combined liver and kidney transplantation must be considered to correct both the hepatic and renal pathology in GSD1 patients.

METHODS

Generation of kidney-specific G6pc knock-out mice

The deficiency in renal G6Pase was obtained by specific deletion of *G6pc* exon 3 in the kidney using a CRE-lox strategy, by crossing B6.G6pc$^{ex3lox/w}$ mice[26] with transgenic mice expressing an inducible CRE^{ERT2} recombinase under the control of the Kap promoter to confer kidney-specific expression (B6.Kap$^{creERT2/w}$)[27]. B6.Kap$^{creERT2/w}$ mice expressed recombinant CRE^{ERT2} recombinase (fused to a mutated ligand-binding domain of the estrogen receptor resulting in a tamoxifen-dependent CRE activity[60,61]) specifically in the proximal convoluted tubules of the kidney cortex. To induce the excision of *G6pc* exon 3 in the kidneys, adult male (6-8 weeks old) B6.G6pc$^{lox/lox}$.Kap$^{creERT2/w}$ and C57Bl/6J mice (Charles

Rivers Laboratories) were intraperitoneally injected daily with 1mg of tamoxifen on five consecutive days to obtain K-G6pc$^{-/-}$ and wild-type (WT) mice, respectively. Mice were housed in the animal facility of Lyon 1 University under temperature controlled (22°C) conditions and with a 12/12 h light/dark cycle. Mice had free access to water and standard chow. Fasted mice were provided with continuous access to water. Mice were studied six months after tamoxifen treatment. Mouse genotypes were determined using PCR from genomic DNA extracted in PCR Direct Lysis Buffer (Euromedex)[26].

Metabolic studies

Mice were housed in individual metabolic cages (Ugo Basile, Comerio, Italy) for 24 h for acclimation before the experimentation. Urine was collected during the 24 h. Urine creatinine, urea, glucose and electrolytes were measured in an automatic analyzer (Konelab, Thermo, France). Albuminuria was assessed using a mouse albumin Elisa kit (Neobiotech) and the uric acid concentration was determined using a colorimetric kit (Biomérieux, Marcy l'Etoile, France). Proteinuria was evaluated using the pyrogallol red-molybdate method. Urine β-hydroxybutyrate was measured with an Abcam colorimetric kit. Urine pH was determined using strips with ΔpH = 0.2.

Blood was withdrawn by submandibular bleeding using a lancet and collected into EDTA or sodium fluoride/oxalate. Blood glucose was measured with an Accu-Check Go glucometer (Roche Diagnostics). Plasma triglycerides, cholesterol, uric acid and lactate concentrations were determined with Biomérieux colorimetric kits. β-hydroxybutyrate concentrations in plasma were assessed with an Abcam colorimetric kit. Plasma blood urea nitrogen levels were measured using a colorimetric kit (BioAssay Systems). Renal glycogen determinations were carried out on frozen tissue homogenates according to the procedure previously described[62].

Gene expression analysis

After 6 h of fasting, mice were killed by cervical dislocation. The liver and kidneys were rapidly removed and frozen using tongs previously chilled in liquid nitrogen. G6Pase activity was assayed at maximal velocity as previously described[5,63,64]. Western blot analyses were carried out using rabbit polyclonal antibodies against G6PC (1:5,000)[8], NPHS2 (Abcam, 1:5,000), nephrin (Abcam, 1:5,000), E-cadherin (Cell Signaling, 1:1,000), β-catenin (Cell Signaling, 1:1,000) and vimentin (Cell Signaling, 1:1,000). Total RNA was isolated from the kidneys according to the Trizol protocol (Invitrogen). Reverse transcription and real-time PCR were performed using sequence-specific primers (Supplemental Table 1) in a Mastercycler Realplex (Eppendorf, Le Pecq, France)[65]. The mouse ribosomal protein mL19 transcript (*Rpl19*) was used as reference.

Histological analysis

Half of the kidney was fixed in 10% formalin and embedded in paraffin or snap frozen in isopentane, cooled in liquid nitrogen and embedded in OCT (Sakura Finetek, AT Zoeterwoude, NL). For formalin-fixed, paraffin-embedded tissues, 4 µm thick sections were cut and stained with hematoxylin and eosin (H&E) or periodic acid Schiff (PAS) staining. Cross-sections (10 µm thick) were obtained from frozen, OCT-embedded tissues and stained with Sudan red.

Immunohistochemical analyses were performed on tissue sections after heat-mediated antigen retrieval using sodium citrate buffer (pH 6.0). Endogenous tissue peroxidases were inhibited with 3% hydrogen peroxide in water for 5 min. The sections were incubated overnight at 4°C with a purified rabbit anti-G6PC antibody (diluted 1:1000) and with biotinylated anti-rabbit IgG antibody (diluted 1:300, Vector). The immune complexes were visualized using a Dako kit (LSAB+, system-HRP, Courtaboeuf, France), and the sections were

counterstained with H&E before mounting[8]. The slides were examined under a Coolscope microscope (Nikon).

Statistical analysis

The results are reported as the mean ± SEM. Significance was determined by an unpaired 2-tailed Student's t-test. Differences were considered to be statistically significant at $p < 0.05$.

Study approval

All of the procedures were performed in accordance with the principles and guidelines established by the European Convention for the Protection of Laboratory Animals. The regional animal care committee (C2EA-55, Université Lyon 1, Lyon) approved all experiments.

DISCLOSURE: The authors declare that there is no conflict of interest.

REFERENCES

1. Shelly LL, Lei KJ, Pan CJ, *et al.* Isolation of the gene for murine glucose-6-phosphatase, the enzyme deficient in glycogen storage disease type 1A. *J. Biol. Chem.* 1993; **268**: 21482–21485.

2. Cori GT, Cori CF. Glucose-6-phosphatase of the liver in glycogen storage disease. *J. Biol. Chem.* 1952; **199**: 661–667.

3. Lei KJ, Shelly LL, Pan CJ, *et al.* Mutations in the glucose-6-phosphatase gene that cause glycogen storage disease type 1a. *Science* 1993; **262**: 580–583.

4. Bruni N, Rajas F, Montano S, *et al.* Enzymatic characterization of four new mutations in the glucose-6 phosphatase (G6PC) gene which cause glycogen storage disease type 1a. *Ann. Hum. Genet.* 1999; **63**: 141–146.

5. Rajas F, Bruni N, Montano S, *et al.* The glucose-6 phosphatase gene is expressed in human and rat small intestine: regulation of expression in fasted and diabetic rats. *Gastroenterology* 1999; **117**: 132–139.

6. Mithieux G, Rajas F, Gautier-Stein A. A novel role for glucose 6-phosphatase in the small intestine in the control of glucose homeostasis. *J. Biol. Chem.* 2004; **279**: 44231–44234.

7. Mithieux G, Bady I, Gautier A, *et al.* Induction of control genes in intestinal gluconeogenesis is sequential during fasting and maximal in diabetes. *Am. J. Physiol. Endocrinol. Metab.* 2004; **286**: E370–375.

8. Rajas F, Jourdan-Pineau H, Stefanutti A, *et al.* Immunocytochemical localization of glucose 6-phosphatase and cytosolic phosphoenolpyruvate carboxykinase in gluconeogenic tissues reveals unsuspected metabolic zonation. *Histochem. Cell Biol.* 2007; **127**: 555–565.

9. Chou JY, Matern D, Mansfield BC, *et al.* Type I glycogen storage diseases: disorders of the glucose-6-phosphatase complex. *Curr. Mol. Med.* 2002; **2**: 121–143.

10. Wolfsdorf JI, Crigler JF Jr. Effect of continuous glucose therapy begun in infancy on the long-term clinical course of patients with type I glycogen storage disease. *J. Pediatr. Gastroenterol. Nutr.* 1999; **29**: 136–143.

11. Weinstein DA, Wolfsdorf JI. Effect of continuous glucose therapy with uncooked cornstarch on the long-term clinical course of type 1a glycogen storage disease. *Eur. J. Pediatr.* 2002; **161 Suppl 1**: S35–39.

12. Rake JP, Visser G, Labrune P, *et al.* Guidelines for management of glycogen storage disease type I - European Study on Glycogen Storage Disease Type I (ESGSD I). *Eur. J. Pediatr.* 2002; **161 Suppl 1**: S112–119.

13. Froissart R, Piraud M, Boudjemline AM, *et al.* Glucose-6-phosphatase deficiency. *Orphanet J Rare Dis* 2011; **6**: 27.

14. Chou JY, Jun HS, Mansfield BC. Glycogen storage disease type I and G6Pase-β deficiency: etiology and therapy. *Nat Rev Endocrinol* 2010; **6**: 676–688.

15. Chen YT, Coleman RA, Scheinman JI, *et al.* Renal disease in type I glycogen storage disease. *N. Engl. J. Med.* 1988; **318**: 7–11.

16. Baker L, Dahlem S, Goldfarb S, *et al.* Hyperfiltration and renal disease in glycogen storage disease, type I. *Kidney Int.* 1989; **35**: 1345–1350.

17. Chen YT. Type I glycogen storage disease: kidney involvement, pathogenesis and its treatment. *Pediatr. Nephrol.* 1991; **5**: 71–76.

18. Reitsma-Bierens WC, Smit GP, Troelstra JA. Renal function and kidney size in glycogen storage disease type I. *Pediatr. Nephrol.* 1992; **6**: 236–238.

19. Reitsma-Bierens WC. Renal complications in glycogen storage disease type I. *Eur. J. Pediatr.* 1993; **152 Suppl 1**: S60–62.

20. Lee PJ, Dalton RN, Shah V, *et al.* Glomerular and tubular function in glycogen storage disease. *Pediatr. Nephrol.* 1995; **9**: 705–710.

21. Yiu WH, Pan C-J, Ruef RA, *et al.* Angiotensin mediates renal fibrosis in the nephropathy of glycogen storage disease type Ia. *Kidney Int.* 2008; **73**: 716–723.

22. Yiu WH, Mead PA, Jun HS, *et al.* Oxidative stress mediates nephropathy in type Ia glycogen storage disease. *Lab. Invest.* 2010; **90**: 620–629.

23. Melis D, Parenti G, Gatti R, *et al.* Efficacy of ACE-inhibitor therapy on renal disease in glycogen storage disease type 1: a multicentre retrospective study. *Clin. Endocrinol. (Oxf)* 2005; **63**: 19–25.

24. Martens DHJ, Rake JP, Navis G, *et al.* Renal function in glycogen storage disease type I, natural course, and renopreservative effects of ACE inhibition. *Clin J Am Soc Nephrol* 2009; **4**: 1741–1746.

25. Lei KJ, Chen H, Pan CJ, *et al.* Glucose-6-phosphatase dependent substrate transport in the glycogen storage disease type-1a mouse. *Nat. Genet.* 1996; **13**: 203–209.

26. Mutel E, Abdul-Wahed A, Ramamonjisoa N, *et al.* Targeted deletion of liver glucose-6 phosphatase mimics glycogen storage disease type 1a including development of multiple adenomas. *J. Hepatol.* 2011; **54**: 529–537.

27. Li H, Zhou X, Davis DR, *et al.* An androgen-inducible proximal tubule-specific Cre recombinase transgenic model. *Am. J. Physiol. Renal Physiol.* 2008; **294**: F1481–1486.

28. Carew RM, Wang B, Kantharidis P. The role of EMT in renal fibrosis. *Cell Tissue Res.* 2012; **347**: 103–116.

29. Urushihara M, Kagami S, Ito M, *et al.* Transforming growth factor-beta in renal disease with glycogen storage disease I. *Pediatr. Nephrol.* 2004; **19**: 676–678.

30. Chen YT, Scheinman JI, Park HK, *et al.* Amelioration of proximal renal tubular dysfunction in type I glycogen storage disease with dietary therapy. *N. Engl. J. Med.* 1990; **323**: 590–593.

31. Matsuo N, Tsuchiya Y, Cho H, *et al.* Proximal renal tubular acidosis in a child with type 1 glycogen storage disease. *Acta Paediatr Scand* 1986; **75**: 332–335.

32. Weinstein DA, Somers MJ, Wolfsdorf JI. Decreased urinary citrate excretion in type 1a glycogen storage disease. *J. Pediatr.* 2001; **138**: 378–382.

33. Emmett M, Narins RG. Renal tranplantation in type 1 glycogenosis. Failure to improve glucose metabolism. *JAMA* 1978; **239**: 1642–1644.

34. Faivre L, Houssin D, Valayer J, *et al.* Long-term outcome of liver transplantation in patients with glycogen storage disease type Ia. *J. Inherit. Metab. Dis.* 1999; **22**: 723–732.

35. Labrune P. Glycogen storage disease type I: indications for liver and/or kidney transplantation. *Eur. J. Pediatr.* 2002; **161 Suppl 1**: S53–55.

36. Reddy SK, Austin SL, Spencer-Manzon M, *et al.* Liver transplantation for glycogen storage disease type Ia. *J. Hepatol.* 2009; **51**: 483–490.

37. Davis MK, Weinstein DA. Liver transplantation in children with glycogen storage disease: controversies and evaluation of the risk/benefit of this procedure. *Pediatr Transplant* 2008; **12**: 137–145.

38. Jankauskiene A, Druskis V, Laurinavicius A. Cyclosporine nephrotoxicity: associated allograft dysfunction at low trough concentration. *Clin. Nephrol.* 2001; **56**: S27–29.

39. Panaro F, Andorno E, Basile G, *et al.* Simultaneous liver-kidney transplantation for glycogen storage disease type IA (von Gierke's disease). *Transplant. Proc.* 2004; **36**: 1483–1484.

40. Belingheri M, Ghio L, Sala A, *et al.* Combined liver-kidney transplantation in glycogen storage disease Ia: a case beyond the guidelines. *Liver Transpl.* 2007; **13**: 762–764.

41. Yiu WH, Lee YM, Peng W-T, *et al.* Complete normalization of hepatic G6PC deficiency in murine glycogen storage disease type Ia using gene therapy. *Mol. Ther.* 2010; **18**: 1076–1084.

42. Luo X, Hall G, Li S, *et al.* Hepatorenal correction in murine glycogen storage disease type I with a double-stranded adeno-associated virus vector. *Mol. Ther.* 2011; **19**: 1961–1970.

43. Ghosh A, Allamarvdasht M, Pan C-J, *et al.* Long-term correction of murine glycogen storage disease type Ia by recombinant adeno-associated virus-1-mediated gene transfer. *Gene Ther.* 2006; **13**: 321–329.

44. Mundel P, Shankland SJ. Podocyte biology and response to injury. *J. Am. Soc. Nephrol.* 2002; **13**: 3005–3015.

45. Wolf G, Chen S, Ziyadeh FN. From the periphery of the glomerular capillary wall toward the center of disease: podocyte injury comes of age in diabetic nephropathy. *Diabetes* 2005; **54**: 1626–1634.

46. Pagtalunan ME, Miller PL, Jumping-Eagle S, *et al.* Podocyte loss and progressive glomerular injury in type II diabetes. *J. Clin. Invest.* 1997; **99**: 342–348.

47. Dalla Vestra M, Masiero A, Roiter AM, *et al.* Is podocyte injury relevant in diabetic nephropathy? Studies in patients with type 2 diabetes. *Diabetes* 2003; **52**: 1031–1035.

48. Li Y, Kang YS, Dai C, *et al.* Epithelial-to-mesenchymal transition is a potential pathway leading to podocyte dysfunction and proteinuria. *Am. J. Pathol.* 2008; **172**: 299–308.

49. Liu Y. New insights into epithelial-mesenchymal transition in kidney fibrosis. *J. Am. Soc. Nephrol.* 2010; **21**: 212–222.

50. Hills CE, Squires PE. The role of TGF-β and epithelial-to mesenchymal transition in diabetic nephropathy. *Cytokine Growth Factor Rev.* 2011; **22**: 131–139.

51. Obara K, Saito T, Sato H, *et al.* Renal histology in two adult patients with type I glycogen storage disease. *Clin. Nephrol.* 1993; **39**: 59–64.

52. Mundy HR, Lee PJ. Glycogenosis type I and diabetes mellitus: a common mechanism for renal dysfunction? *Med. Hypotheses* 2002; **59**: 110–114.

53. Koya D, King GL. Protein kinase C activation and the development of diabetic complications. *Diabetes* 1998; **47**: 859–866.

54. Bobulescu IA. Renal lipid metabolism and lipotoxicity. *Curr. Opin. Nephrol. Hypertens.* 2010; **19**: 393–402.

55. Sun L, Halaihel N, Zhang W, *et al.* Role of sterol regulatory element-binding protein 1 in regulation of renal lipid metabolism and glomerulosclerosis in diabetes mellitus. *J. Biol. Chem.* 2002; **277**: 18919–18927.

56. Wang Z, Jiang T, Li J, *et al.* Regulation of renal lipid metabolism, lipid accumulation, and glomerulosclerosis in FVBdb/db mice with type 2 diabetes. *Diabetes* 2005; **54**: 2328–2335.

57. Zhang D, Yang H, Kong X, *et al.* Proteomics analysis reveals diabetic kidney as a ketogenic organ in type 2 diabetes. *Am. J. Physiol. Endocrinol. Metab.* 2011; **300**: E287–295.

58. Binkiewicz A, Senior B. Decreased ketogenesis in von Gierke's disease (type I glycogenosis). *J. Pediatr.* 1973; **83**: 973–978.

59. Delaere F, Magnan C, Mithieux G. Hypothalamic integration of portal glucose signals and control of food intake and insulin sensitivity. *Diabetes Metab.* 2010; **36**: 257–262.

60. Feil R, Brocard J, Mascrez B, *et al.* Ligand-activated site-specific recombination in mice. *Proc. Natl. Acad. Sci. U.S.A.* 1996; **93**: 10887–10890.

61. Nagy A. Cre recombinase: the universal reagent for genome tailoring. *Genesis* 2000; **26**: 99–109.

62. Pfleiderer G. Glycogen: determination with amyloglucosidase. In: *Methods of Enzymatic Analysis*.Vol 2. 2nd ed. Verlag-Chemie. Deerfield Beach, FL, US: Bermeyer HU; 1974:59–62.

63. Mithieux G, Daniele N, Payrastre B, *et al.* Liver microsomal glucose-6-phosphatase is competitively inhibited by the lipid products of phosphatidylinositol 3-kinase. *J. Biol. Chem.* 1998; **273**: 17–19.

64. Daniele N, Rajas F, Payrastre B, *et al.* Phosphatidylinositol 3-kinase translocates onto liver endoplasmic reticulum and may account for the inhibition of glucose-6-phosphatase during refeeding. *J. Biol. Chem.* 1999; **274**: 3597–3601.

65. Pillot B, Soty M, Gautier-Stein A, *et al.* Protein feeding promotes redistribution of endogenous glucose production to the kidney and potentiates its suppression by insulin. *Endocrinology* 2009; **150**: 616–624.

ACKNOWLEDGMENTS

We would like to thank the members of Animalerie Lyon Est Conventionnelle et SPF (Université Lyon 1, Faculté Lyon Est, SFR Santé Lyon Est) for animal care and the members of the Anipath platform for histological experiments (Faculté Lyon-Est). Thanks to Dr. Gaëlle Brideau and the members of the Plateforme d'exploration fonctionnelle rénale des Cordeliers (Paris) and Dr. Annie Varennes (Hospices Civils de Lyon, 69500 Bron, France; Université de Lyon) for urine analyses. Thank you to the members of the CECIL platform (Université Lyon 1, Faculté Lyon-Est). We greatly thank Dr. Laurence Dubourg (Laboratoire d'Exploration fonctionnelle rénale et métabolique, Hôpital Edouard Herriot, Lyon) and Prof. Philippe Labrune (Centre de référence Maladies héréditaires du métabolisme hépatique,

Hôpital Antoine Béclère, Clamart, France) for their invaluable help in interpreting the urinary data and advice for the discussion of the data. This work was supported by research grants from the Agence Nationale de la Recherche (ANR11-BSV1-009-01) and the Association Francophone des Glycogénoses.

TITLES AND LEGENDS

Figure 1: Partial deletion of renal *G6pc* in K-G6pc$^{-/-}$ mice.

(A) Kidney-specific excision of *G6pc* exon 3. Genomic PCR analysis of purified DNA from the kidney, liver, intestine, testis and epididymis revealed products of 1189, 1029 and 595 bp corresponding to the floxed, wild-type and excised *G6pc* alleles, respectively. Specific primers were used to amplify a 320 bp *Cre* fragment in K-G6pc$^{-/-}$ mice. (B) Renal G6Pase activity in WT (white bar) and K-G6pc$^{-/-}$ (black bar) mice after 6 h of fasting. The results are expressed as the mean ± SEM (n = 12 mice per group). The top panel shows western-blot analysis of G6PC in WT and K-G6pc$^{-/-}$ kidney homogenates. (C-D) Immunohistochemical analyses of G6PC in the kidneys of WT mice (C and E) and K-G6pc$^{-/-}$ mice (D and F). G: glomeruli, DC: distal convoluted tubules, PC: proximal convoluted tubules.

Figure 2: Nephromegaly and renal glycogen storage in K-G6pc$^{-/-}$ mice.

(A) Kidneys of WT and K-G6pc$^{-/-}$ mice. (B) The weight of two kidneys, (C) the relative weight of the kidneys compared to body mass and (F) renal glycogen content in WT (white bars) and K-G6pc$^{-/-}$ (black bars) mice. (D-E) PAS-stained kidney from WT (D) and K-G6pc$^{-/-}$ mice (E). G: glomeruli, DC: distal convoluted tubules, PC: proximal convoluted tubules. Data were obtained from mice after 6 h of fasting and are expressed as the mean ± SEM (n = 12 mice per group). Significant differences between WT and K-G6pc$^{-/-}$ mice are indicated ($p < 0.001$***).

Figure 3: Morphological alterations and podocyte damage in K-G6pc$^{-/-}$ kidneys.

Histological analyses of hematoxylin-eosin staining from WT (A and C) and K-G6pc$^{-/-}$ kidneys (B and D). Panels C and D correspond to a higher magnification of the kidney cortex

observed in panels A and B, respectively. G: glomeruli, DC: distal convoluted tubules, PC: proximal convoluted tubules. (E) Expression of podocyte marker proteins in the kidneys of WT (white bars) and K-G6pc$^{-/-}$ (black bars) mice. *Nphs2*: Podocin, *Synpo*: Synaptopodin, *Podxl*: Podocalyxin. The mRNA levels are expressed as a ratio relative to the *Rpl19* mRNA level. The results are expressed as the mean ± SEM (n = 5 mice per group). Significant differences between WT and K-G6pc$^{-/-}$ mice are indicated ($p < 0.01$** and $p < 0.001$***). On the right of panel E are western blot analyses of Nephrin, NHPHS2 and GAPDH (control) proteins in WT and K-G6pc$^{-/-}$ kidney homogenates.

Figure 4: Activation of the renin-angiotensin system leading to epithelial-mesenchymal transition and inflammation in K-G6pc$^{-/-}$ kidneys.

Panels A and B: The expression of renin-angiotensin system components (A) and factors involved in epithelial-mesenchymal transition (B) was analyzed in the kidneys of WT (white bars) and K-G6pc$^{-/-}$ (black bars) mice. On the bottom of panel B are western blot analyses of E-cadherin, β1-catenin, Vimentin and GAPDH (control) proteins in WT and K-G6pc$^{-/-}$ kidney homogenates. Panels: C to F: Electron microscopic analyses of glomeruli (C and D) and proximal convoluted tubules (E and F) of WT (C and E) and K-G6pc$^{-/-}$ kidneys (D and F). Panel G: Determination of inflammation in the kidneys of WT (white bars) and K-G6pc$^{-/-}$ (black bars) mice. The mRNA levels are expressed as a ratio relative to the *Rpl19* mRNA level. *Agt*: angiotensinogen, *Tgfb1*: transforming growth factor β1, *Cdh1*: E-cadherin, *ZO1*: tight junction protein ZO-1, *Ctnnb1*: catenin β1, *αSMA*: α2 smooth muscle actin, *PAI1*: plasminogen activator inhibitor type 1, *Tnf*: tumor necrosis factor. The results are expressed as the mean ± SEM (n = 5 mice per group). Significant differences between WT and K-G6pc$^{-/-}$ mice are indicated ($p < 0.01$**).

Figure 5: Altered renal lipid metabolism and lipid deposits in K-G6pc$^{-/-}$ kidneys.

Histological analysis of Sudan red staining from WT (A) and K-G6pc$^{-/-}$ kidneys (B-C). Panel C corresponds to a higher magnification of the lipid deposits showed in panel B. (D) Expression of the main lipogenic genes in the kidneys of WT (white bars) and K-G6pc$^{-/-}$ (black bars) mice. The mRNA levels are expressed as a ratio relative to the *Rpl19* mRNA level. The results are expressed as the mean ± SEM (n = 5 mice per group). Significant differences between WT and K-G6pc$^{-/-}$ mice are indicated ($p < 0.01$**). *Fasn*: fatty acid synthase, *Acaca*: acetyl-coenzyme A carboxylase α, *Scd1*: stearoyl-coenzyme A desaturase 1, *Hmgcr*: 3-hydroxy-3-methylglutaryl coenzyme A reductase, *Srebf1*: sterol regulatory element-binding factor 1, *Srebf2*: sterol regulatory element-binding factor 2, *Chrebp*: carbohydrate-responsive element-binding protein, *Hmgcs2*: 3-hydroxy-3-methylglutaryl coenzyme A synthase 2.

Table 1: Body weight, hepatic and plasmatic parameters of wild-type and K-G6pc$^{-/-}$ mice

Table 2: Urinary parameters of wild-type and K-G6pc$^{-/-}$ mice

Table 1: Body weight, hepatic and plasmatic parameters of wild-type and K-G6pc$^{-/-}$ mice

	WT	K-G6pc$^{-/-}$
Body weight (g)	34 ± 1	32 ± 1
Liver weight (g)	1.4 ± 0.1	1.5 ± 0.1
Hepatic G6Pase activity (U/g prot)	73 ± 9	102 ± 3 **
Glucose (mg/dL)	147 ± 9	158 ± 8
Cholesterol (g/L)	1.2 ± 0.1	1.0 ± 0.1
Triglycerides (g/L)	0.6 ± 0.1	0.6 ± 0.1
Lactate (mM)	2.3 ± 0.3	2.4 ± 0.2
Uric acid (mg/L)	6.2 ± 0.7	11.1 ± 1.0 **
Ketone bodies (mM)	0.6 ± 0.1	0.6 ± 0.1
Blood urea nitrogen (mg/dL)	29.8 ± 1.6	25.7 ± 1.5

Data were obtained from mice after 6 h of fasting and are expressed as the mean ± SEM (n = 8 mice in each group). Significant differences between WT and K-G6pc$^{-/-}$ mice are indicated ($p < 0.01$**).

Table 2: Urinary parameters of wild-type and K-G6pc$^{-/-}$ mice

	WT	K-G6pc$^{-/-}$
Urinary volume (mL)	1.4 ± 0.1	1.7 ± 0.3
Urinary pH	7.1 ± 0.2	5.8 ± 0.1 **
β-HB (µmol/24h)	0.84 ± 0.05	1.03 ± 0.15
Uric acid (mg/24h)	0.13 ± 0.01	0.35 ± 0.13 *
Urea (mmol/24h)	1.8 ± 0.2	2.3 ± 0.4
Creatinine (µmol/24h)	8.0 ± 0.5	9.3 ± 1.2
Albumin (µg/24h)	19 ± 2	53 ± 7 ***
Proteins (mg/24h)	7.1 ± 0.7	7.2 ± 0.9
Glucose (mg/24h)	1.8 ± 0.1	2.3 ± 0.3
Magnesium (µmol/24h)	28 ± 3	43 ± 7 *
Phosphate (µmol/24h)	29 ± 6	60 ± 11 **
Calcium (µmol/24h)	2.0 ± 0.3	2.4 ± 0.3
Chloride (µmol/24h)	393 ± 53	437 ± 58
Sodium (µmol/24h)	288 ± 26	333 ± 31
Potassium (µmol/24h)	435 ± 42	503 ± 36
Citrate (µmol/24h)	26 ± 3	56 ± 9*
Oxalate (µmol/24h)	1.9 ± 0.1	2.2 ± 0.2

The data were obtained from fed mice and are expressed as the mean ± SEM (n = 8 mice in each group). Significant differences between WT and K-G6pc$^{-/-}$ mice are indicated ($p < 0.05$*, $p < 0.01$** and $p < 0.001$***).

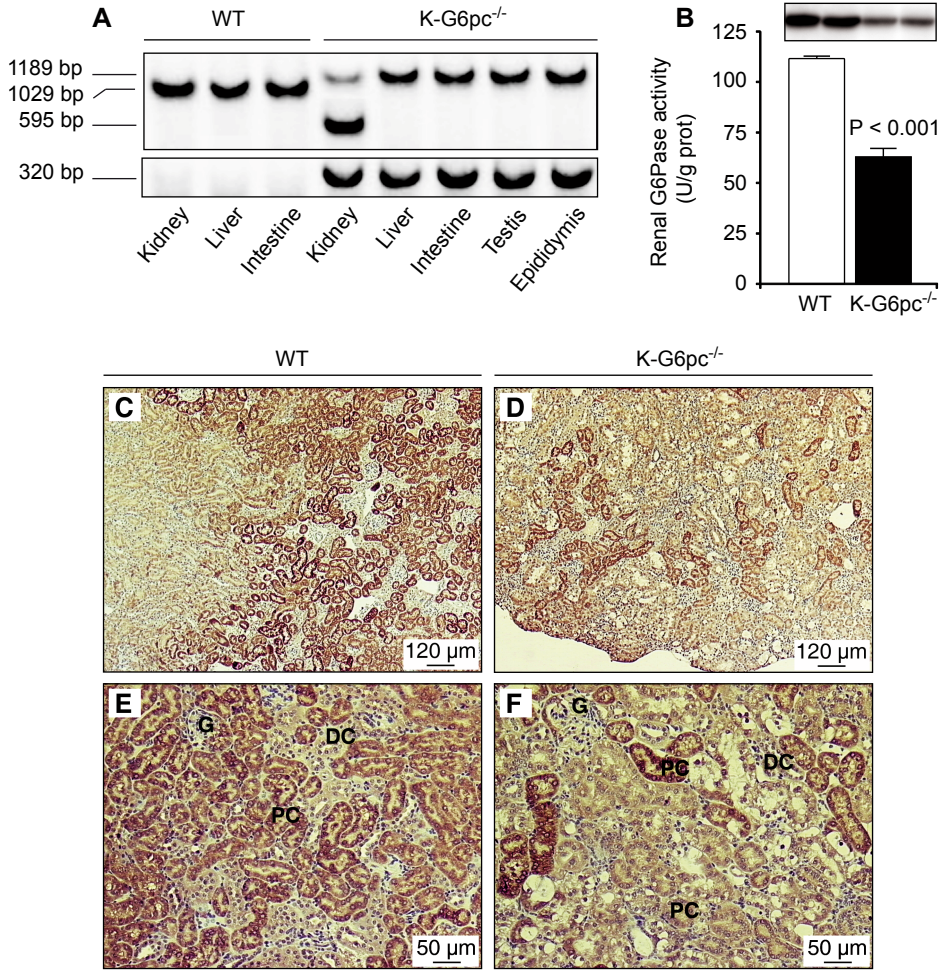
A
WT
K-G6pc-/-
1189 bp
1029 bp
595 bp
320 bp
Kidney
Liver
Intestine
Kidney
Liver
Intestine
Testis
Epididymis
B
125
100
75
50
25
0
Renal G6Pase activity
(U/g prot)
P < 0.001
WT
K-G6pc-/-
WT
K-G6pc-/-
C
120 µm
D
120 µm
E
G
DC
PC
50 µm
F
G
PC
DC
PC
50 µm

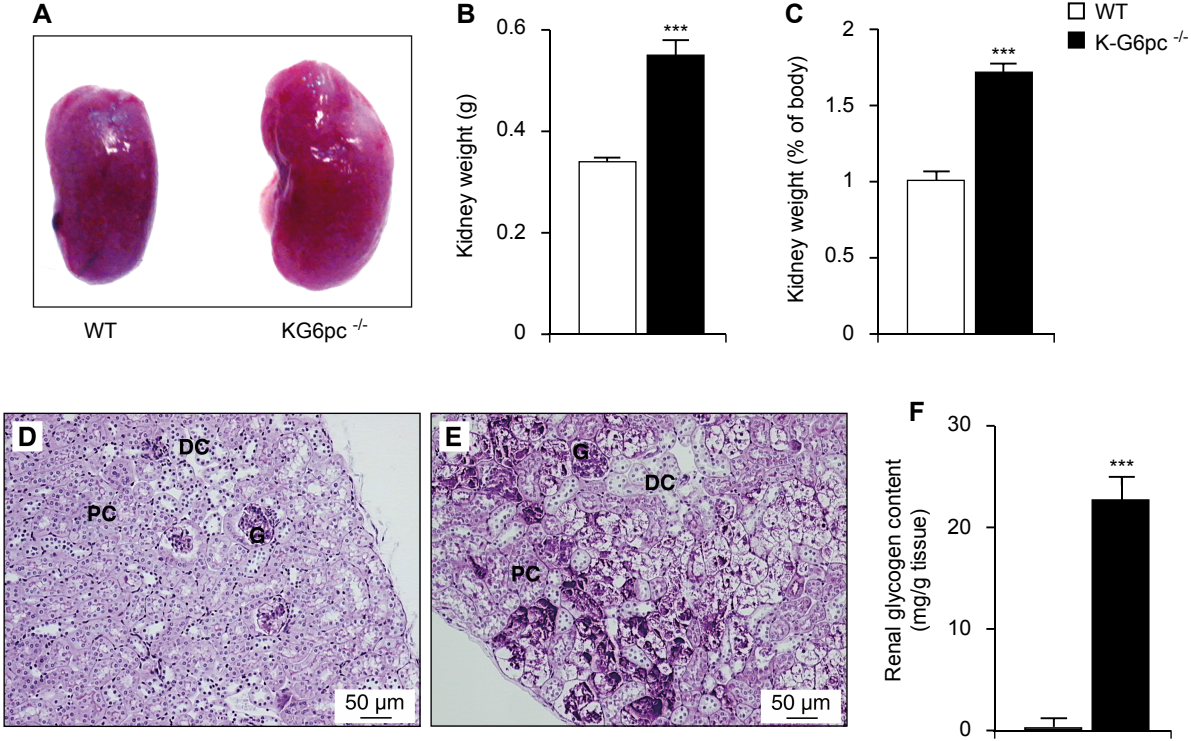
A
WT
KG6pc -/-
B
Kidney weight (g)
0.6
0.4
0.2
0
***
C
Kidney weight (% of body)
2
1.5
1
0.5
0
***
WT
K-G6pc -/-
D
DC
PC
G
50 µm
E
G
DC
PC
50 µm
F
Renal glycogen content (mg/g tissue)
30
20
10
0
***

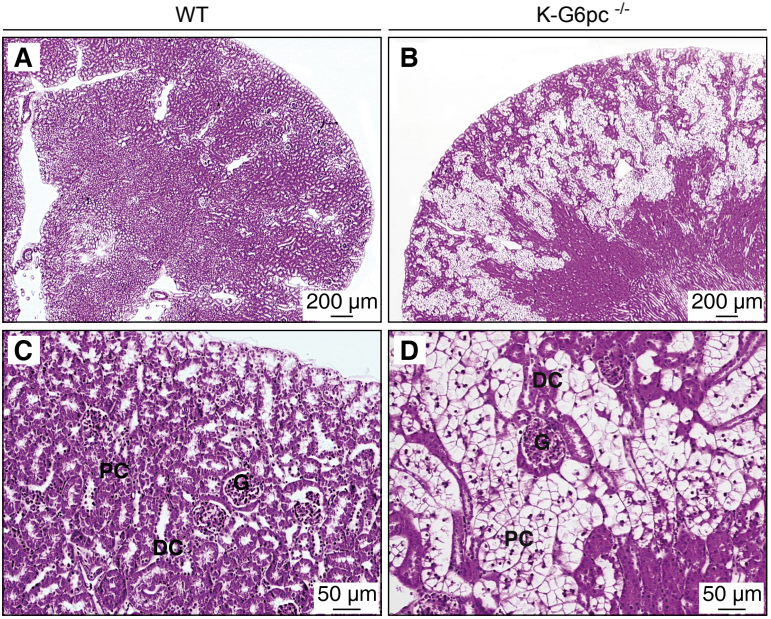
WT
K-G6pc -/-
A
B
200 µm
200 µm
C
D
PC
G
DC
DC
G
PC
50 µm
50 µm

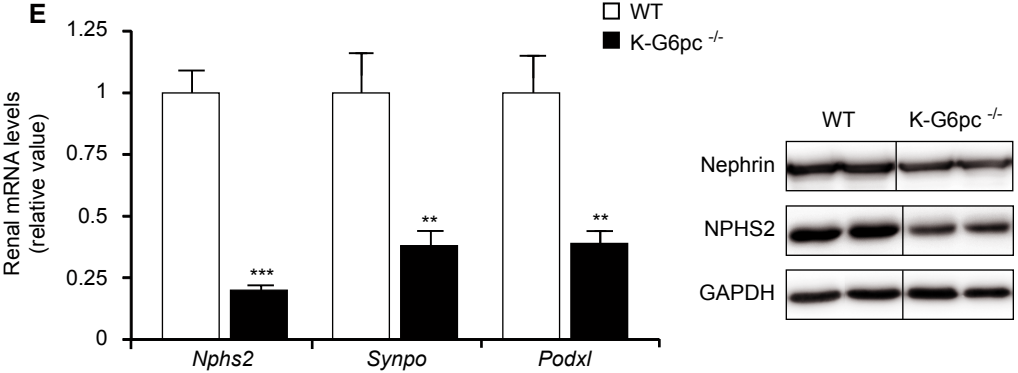
E
WT
K-G6pc -/-
Renal mRNA levels
(relative value)
1.25
1
0.75
0.5
0.25
0
***
**
**
Nphs2
Synpo
Podxl
WT
K-G6pc -/-
Nephrin
NPHS2
GAPDH

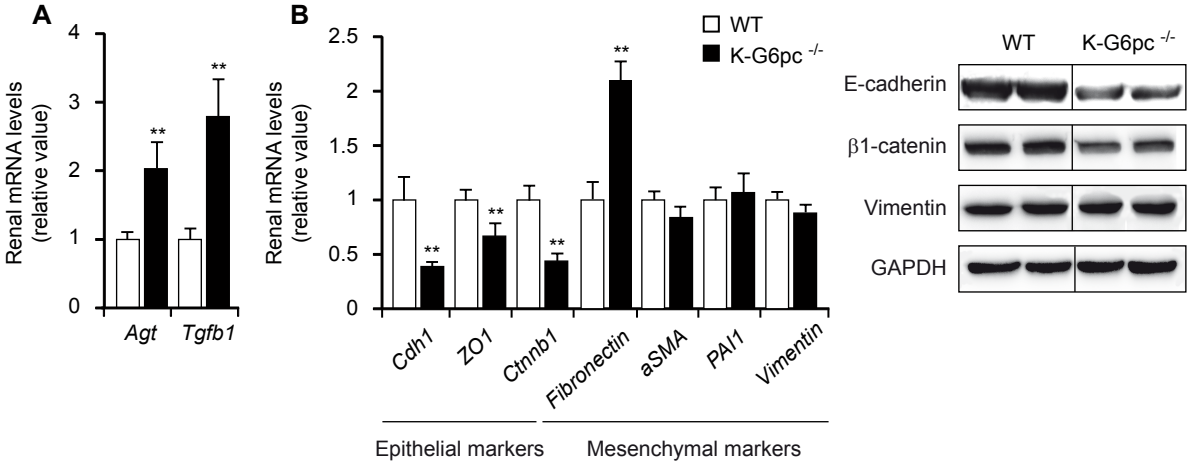
A
Renal mRNA levels (relative value)
4
3
2
1
0
**
**
Agt
Tgfb1
B
Renal mRNA levels (relative value)
2.5
2
1.5
1
0.5
0
WT
K-G6pc -/-
**
**
**
**
Cdh1
ZO1
Ctnnb1
Fibronectin
aSMA
PAI1
Vimentin
Epithelial markers
Mesenchymal markers
WT
K-G6pc -/-
E-cadherin
β1-catenin
Vimentin
GAPDH

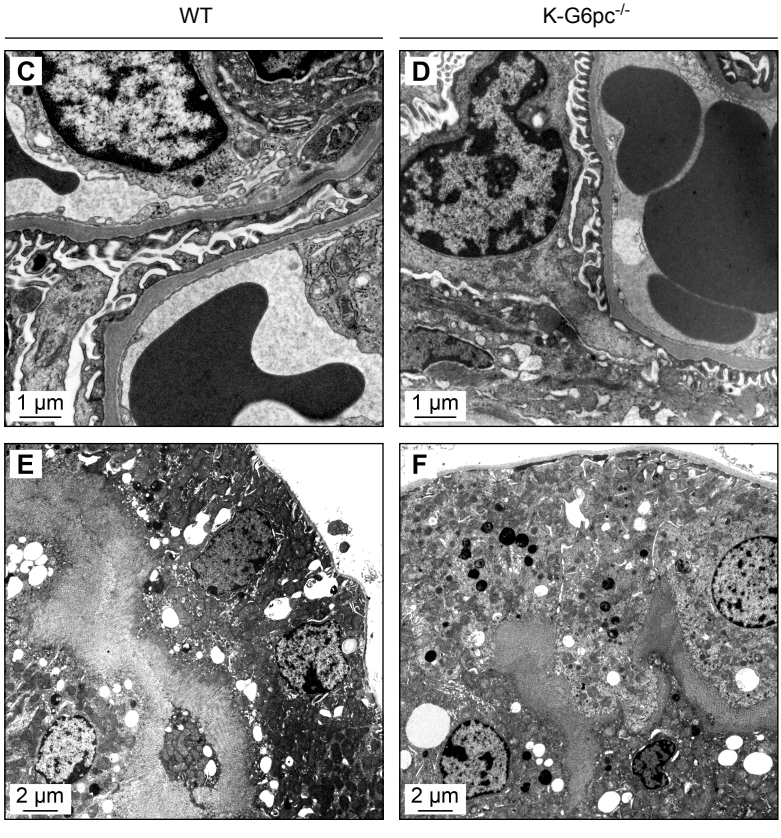
WT
K-G6pc-/-
C
1 μm
D
1 μm
E
2 μm
F
2 μm

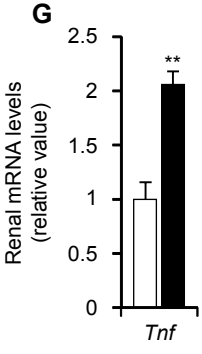
G
Renal mRNA levels (relative value)
2.5
2
1.5
1
0.5
0
**
Tnf

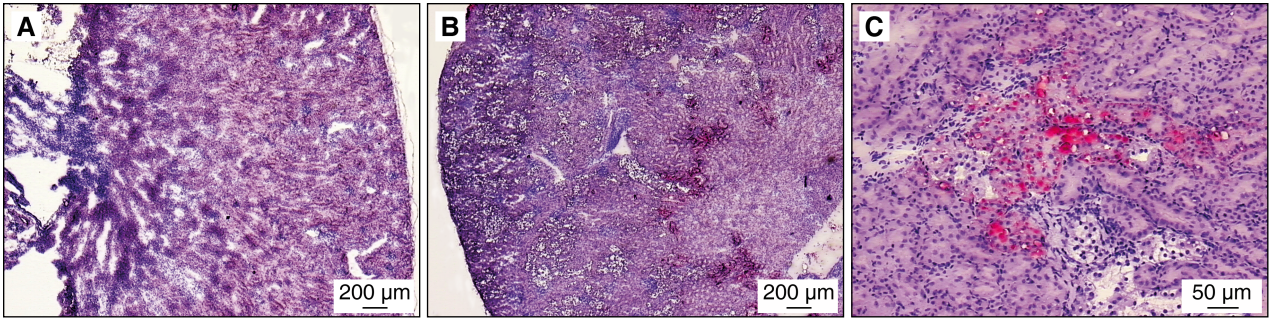
A
200 μm
B
200 μm
C
50 μm

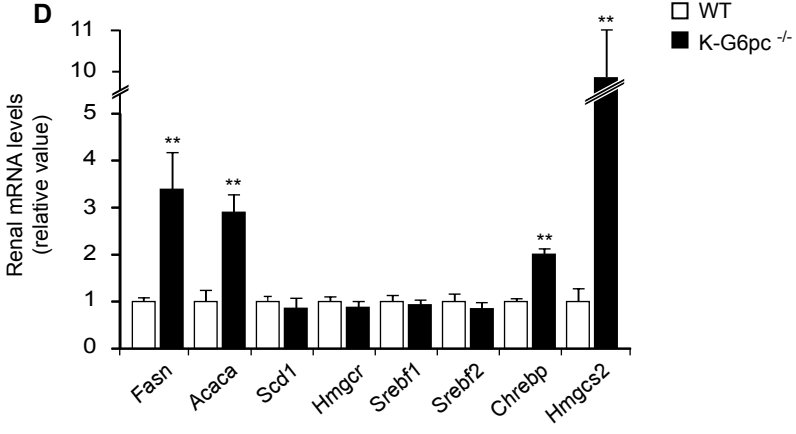
D
WT
K-G6pc -/-
Renal mRNA levels
(relative value)
11
10
5
4
3
2
1
0
**
Fasn
Acaca
Scd1
Hmgcr
Srebf1
Srebf2
Chrebp
Hmgcs2